ND-stretching vibrational energy relaxation of NH_2D in liquid-to-supercritical ammonia studied by femtosecond midinfrared spectroscopy

Tim Schäfer and Dirk Schwarzer
Arbeitsgruppe Reaktionsdynamik, Max-Planck-Institut für Biophysikalische Chemie, Am Fassberg 11, 37077 Göttingen, Germany

Jörg Lindner and Peter Vöhringer[a)]
Abteilung für Molekulare Physikalische Chemie, Institut für Physikalische und Theoretische Chemie, Rheinische Friedrich-Wilhelms-Universität, Wegelerstraße 12, 53115 Bonn, Germany

(Received 9 October 2007; accepted 29 November 2007; published online 8 February 2008)

Femtosecond midinfrared pump-probe spectroscopy was carried out to explore the dynamics of vibrational energy relaxation of NH_2D in fluid ammonia NH_3. The ND-stretching fundamental of the partially deuterated solute NH_2D was excited by femtosecond pulses centered at 2450 cm^{-1}, and both the ground-state bleach and the anharmonically shifted transient absorption of the same vibration was probed. The temperature of the sample was varied between 230 and 450 K, while the pressure was tuned from 10 to 1500 bar, thereby entering both the liquid and the supercritical phase of the fluid solution. The density and temperature dependence of the ND-stretching lifetime suggests that hydrogen bonding is of negligible importance for vibrational energy relaxation. Rather, the energy transfer dynamics can be understood qualitatively in terms of a simple Landau-Teller description for vibrational energy relaxation using molecular dynamics simulations to estimate the spectral density of the fluctuating forces exerted by a weakly interacting Lennard-Jones solvent (NH_3) onto the vibrationally excited solute (NH_2D). © *2008 American Institute of Physics*. [DOI: 10.1063/1.2827464]

INTRODUCTION

Liquid ammonia is often cited in chemistry textbooks as an example for associated liquids forming extended networks of hydrogen bonds (H-bond) similar to water.[1,2] This notion stems from the fact that in addition to their three hydrogen atoms, NH_3 molecules exhibit a lone electron pair. Just like in water, these features render ammonia molecules potential H-bond donors and H-bond acceptors at the same time.

Indeed, from x-ray crystallography,[3,4] it is known that in solid ammonia, each NH_3 molecule is hydrogen bonded to six nearest neighbors, thereby acting simultaneously as a triple H donor and a triple H acceptor with a length $r(N\cdots H)$ of the H bridge of 2.40 Å at an interparticle distance of 3.38 Å. Similarly, ammonia dimers $(NH_3)_2$ in the gas phase[5,6] are held together at a $N\cdots N$ distance of 3.35 Å by a slightly bent hydrogen bond with a dissociation energy of smaller than 12 kJ/mol. Therefore, ammonia dimers classify as moderately strong H-bonded complexes as compared to their H_2O or HF counterparts, whose binding energies are as nearly twice as high at significantly shorter lengths of the hydrogen bridge.[7,8] On the other hand, the binding energy of heterodimers of water and ammonia[9] is approximately 30% larger than that of H_2O homodimers, indicating that albeit being weak H-bond donors, NH_3 molecules can act in the gas phase as very strong H-bond acceptors.

In contrast to the solid or the gaseous phase, evidence for hydrogen bonding in the liquid state is much more difficult to obtain. To date, essentially only two microscopic experimental approaches have been exploited to characterize the importance of hydrogen bonding in liquid NH_3, namely, diffraction experiments such as x-ray[10–12] and neutron[13–15] scattering, on the one hand, and linear vibrational spectroscopies such as infrared (IR) absorption[16] and Raman scattering,[17,18] on the other hand. By studying the density dependence of the vibrational spectra of fluid NH_3 in the NH-stretching spectral region, Buback[16] conjectured that hydrogen bonding is insignificant at and above room temperature and, in particular, under supercritical conditions.

Early x-ray diffraction studies on liquid NH_3 were carried out by Narten[10] and complementary neutron scattering was performed by Chieux and Bertagnolli.[13] Both sets of data were used to extract the nitrogen-nitrogen radial distribution function from which the existence of hydrogen bonds was inferred, in particular, for the fluid at sufficiently low temperatures. To remove the ambiguities associated with atom-atom pair correlation functions from x-ray and neutron scattering, Ricci *et al.*[19] as well as Thompson *et al.*[15] extended neutron scattering experiments to the ammonia isotopomer ND_3 and its equimolar mixture with NH_3. The isotopic substitution enables an extraction of the three individual partial radial distribution functions $g_{NN}(r)$, $g_{NH}(r)$, and $g_{HH}(r)$.

For temperatures below 273 K, some degree of hydrogen bonding was found, yet the scattering data suggest that

[a)]Author to whom correspondence should be addressed. Electronic mail: p.voehringer@uni-bonn.de

in contrast to liquid water, no extended intermolecular H-bond network is supported in liquid NH_3.[19] The ammonia molecules experience orientational correlations such that an excess of particles have their hydrogen atoms directed toward the lone electron pair of a neighboring particle.[19] However, the number of NH_3 molecules in the first solvation shell was estimated to be ~14, indicating a very tight packing of the liquid governed by van-der-Waals-type forces rather than hydrogen bonding.[19] Only a weak shoulder in the N–H partial distribution function due to H-bonded pairs was identified whose radial integral implied an average number of hydrogen bonds of merely 2 per N atom.

Since in light of these results, the relative number of neighboring H atoms (2 out of ~42) is much smaller than in liquid H_2O (4 out of 8), it seems plausible to argue that liquid ammonia does not belong to the group of strongly associated liquids even at low temperatures. Modern computer simulations based on Car-Parinello *ab initio* molecular dynamics[20] and mixed quantum/classical molecular dynamics[21] support such an assignment of liquid NH_3 to weakly associated fluids.

In parallel to these experimental and theoretical efforts primarily designed to explore the structure of H-bonded liquids, modern femtosecond time-resolved spectroscopies have recently been able to uncover unprecedented detail regarding molecular dynamical phenomena in such systems,[22] in particular, in liquid water.[23] Ultrafast nonresonant Raman spectroscopies[24,25] were used to monitor intermolecular motions such as diffusive reorientations, as well as coherently driven restricted translations and hindered rotations in liquid H_2O. These degrees of freedom are directly linked to hydrogen bond motion. Hence, combined with elaborate line shape analyses, such intermolecular spectra were used to provide rough estimates for the lifetime of hydrogen bonds within the three-dimensional random network.[25]

Ultrafast resonant mid-IR spectroscopy on liquid H_2O has focused on the dynamics of vibrational energy transfer following an initial stretching mode excitation.[22,26] Multidimensional variants of mid-IR spectroscopy[27] were used to quantify the dynamics of vibrational spectral diffusion within the OH-stretching resonance of liquid water, which are directly connected to the random fluctuations of its H-bond network both in space and time.

Recently, we have been able to carry out femtosecond mid-IR pump-probe spectroscopy in the OH-stretching region of the partially deuterated water species HOD dissolved in liquid-to-supercritical heavy water.[28,29] The combined temperature and density dependence of the lifetime of the OH-stretching excited state enabled us to disentangle the dynamical interrelation between energy transfer and spectral diffusion dynamics. An empirical correlation between the rate coefficient for vibrational energy transfer and the dielectric constant of the medium was found, which was taken as a quantitative and independent measure for the average hydrogen bond connectivity of water and its dependence on the thermodynamic state variables, temperature and density.[28,29]

To our knowledge, equivalent femtosecond time-resolved vibrational spectroscopies have not yet been performed on ammonia. To test the significance of hydrogen bonding for vibrational relaxation dynamics in this apparently weakly associated fluid and to provide a direct comparison to our previous studies on fluid water, we decided to carry out conventional mid-IR pump-probe spectroscopy on the stretching vibrations in liquid-to-supercritical ammonia. Unfortunately, the NH-stretching region of NH_3 is heavily perturbed by strong Fermi coupling[30–34] between the stretching fundamental, ν_1, and the first overtone of the antisymmetrical bending mode, $2\nu_4$, as evidenced by the appearance of two NH-stretching bands in the isotropic Raman spectrum of NH_3 rather than one.[17]

To avoid this additional complexity, partial deuteration can be used to lift those Fermi resonances[33,34] and to provide highly diluted solute vibrations that are spectroscopically distinct from those of the solvent. Here, we report on the relaxation dynamics of the ND-stretching vibration of the monodeuterated ammonia species NH_2D (the solute) in liquid-to-supercritical ammonia, NH_3 (the solvent). In addition, the partial deuteration has the advantage to avoid transient heating effects[35] and to suppress energy delocalization phenomena,[36] both of which give rise to additional signal contributions when isotopically pure liquids are studied.

EXPERIMENT

Femtosecond mid-IR pump-probe experiments were carried out with a homebuilt ultrafast laser system based on an Er-fiber/Ti-sapphire chirped-pulse amplifier equipped with two independently tunable optical parametric amplifiers (OPAs). The signal and idler output of each OPA were used for generation of mid-IR radiation through difference frequency generation (DFG) in type-I $AgGaS_2$. The laser system provides a 1 kHz train of temporally synchronized pairs of ultrafast mid-IR pulses, each pulse within the pair is independently tunable from roughly 3600 to 1100 cm^{-1} with durations as short as 150 fs and energies as high as 5 μJ.

For referenced signal detection, the mid-IR output of one of the OPA/DFG devices was split into two replicas, i.e., into a reference and a probe pulse. The remaining OPA/DFG combination served as the pump pulse source. The synchronized pump and probe pulses were spatially overlapped inside a high-pressure sample cell and their relative time delay was adjusted by a computer controlled optical delay line. The relative pump-probe polarization was set to magic angle to eliminate signal contributions arising from reorientational motion of the NH_2D molecules. Behind the sample, the probe and reference pulses were fed into a 0.2 m polychromator whose exit plane was outfitted with a 2×32 pixel HgCdTe detector for frequency resolved detection.

The sample was prepared by mixing NH_3 (Aldrich, 99.99% purity) with 2%–5% of ND_3 (Euriso-top, 99% deuteration grade) in a gas tank. Rapid isotope exchange yields fluid mixtures composed of 5.8%–13.5% NH_2D in an excess of NH_3 serving as the solvent. The fraction of the undesired isotopomer ND_2H in the mixture was 0.1%–0.7% and always $\leqslant$5% of the NH_2D content. The mixture was subsequently transferred and compressed into the high-pressure cell, which was equipped with sapphire windows for spectroscopic experiments. Its optical path length was 0.5 mm to

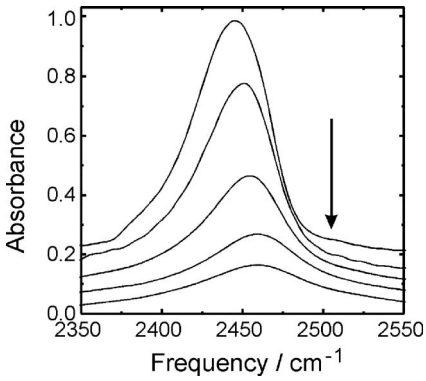

FIG. 1. Linear midinfrared absorption spectra in the ND-stretching region of NH_2D dissolved in NH_3 for the following thermodynamic conditions (from top to bottom): (213 K, 15 bar, 42.4 mol/l), (273 K, 1000 bar, 40.6 mol/l), (323 K, 500 bar, 35.9 mol/l), (373 K, 80 bar, 27.1 mol/l), and (425 K, 670 bar, 29.4 mol/l). For clarity, the spectra have been shifted vertically. All spectra are normalized to constant NH_2D concentration. The vertical arrow indicates the spectral position of the ND-stretching resonance as observed in high-resolution gas-phase studies.

yield a sample optical density of around 0.3–0.5 at the maximum of the ND-stretching absorption of NH_2D. Thermodynamic data of fluid ammonia were taken from Ref. 37.

RESULTS AND DISCUSSION

Linear spectroscopy

Linear mid-IR absorption spectra in the NH-stretching spectral region of NH_2D in fluid NH_3 are shown in Fig. 1 for representative densities of the mixture. All spectra were normalized to the concentration of the NH_2D solute, i.e., the absorbance was scaled to represent a relative molar extinction coefficient of the solute. The vibrational spectra of the various isotopomers of ammonia monomers were recently explored in the gas phase by Snels *et al.*[32,33] and in cryogenic solid-state matrices[34,38–40] using high-resolution Fourier-transform IR spectroscopy. For our solute, NH_2D, the ND-stretching mode, ν_1, was found in the gas phase[32,33] at 2506 cm^{-1}, as represented in Fig. 1 by the vertical arrow.

The spectral bandwidth of the ND-stretching resonance is about 60 cm^{-1}, which is more than twice as narrow as compared to the OD-stretching resonance of the partially deuterated water species HOD in H_2O at similar densities.[28,29] Also, the magnitude of ~50 cm^{-1} for the redshift of the ND resonance in the fluid relative to the gas phase is rather small compared to water under comparable thermodynamic conditions. Similarly, the overall solvent density dependence of the ND-stretching resonance frequency is also extremely small compared to water and can be linearly approximated in the interval of $0.5 \leqslant \rho$ in g cm^{-3} $\leqslant 0.7$ by roughly -1.4 cm^{-1}/M.

Calculating the mean interparticle distance in the fluid from $\langle r \rangle = (M/\rho N_L)^{1/3}$, where N_L is Avogadro's number, this density dependence can be converted into a N–H···N distance dependence of the ND frequency by using $(\Delta\tilde{\nu}/\Delta\langle r\rangle) = -3M/(N_L\langle r\rangle^4)(\Delta\tilde{\nu}/\Delta\rho)$. The density interval quoted above corresponds to a distance interval that is centered at around $\langle r\rangle = 3.64$ Å. From this, we find that $(\Delta\tilde{\nu}/\Delta\langle r\rangle)$ equals 40 $cm^{-1}/Å$ for NH_2D in NH_3.

Novak[41] has classified the strength of hydrogen bonds by compiling experimental data for the spectral position of the (OH and NH) stretching resonance of a large number of hydrogen-bonded systems in the solid phase. Such a classification was justified by arbitrarily dividing the $\tilde{\nu}(\langle r\rangle)$ correlation into three distinct regimes with slopes $(\Delta\tilde{\nu}/\Delta\langle r\rangle) = 12\,000$ $cm^{-1}/Å$ (strongly H-bonded systems, $\langle r\rangle \leqslant 2.6$ Å), $(\Delta\tilde{\nu}/\Delta\langle r\rangle) = 5000$ $cm^{-1}/Å$ (intermediate cases), and $(\Delta\tilde{\nu}/\Delta\langle r\rangle) = 1500$ $cm^{-1}/Å$ (weak H bonds, $\langle r\rangle \geqslant 2.7$ Å).[41]

According to Novak's classification and the distance dependence of the ND-stretching frequency reported herein, ammonia would not even qualify as a weakly hydrogen-bonded system even if one took into account a correction for the isotope shift required for our deuterated solute. However, such a conclusion would have to be drawn for water also, where a value of roughly 30 $cm^{-1}/Å$ can be identified along a supercritical isotherm of ~700 K.[28,29] The discrepancy of two orders of magnitude between the $(\Delta\tilde{\nu}/\Delta\langle r\rangle)$ values reported here and by Novak is of course due to the fact that the packing forces in solids are completely different as compared to the liquid or the supercritical phase. The influence of the thermodynamic state becomes particularly obvious by the observation of a discontinuity of the density-dependent stretching frequency at the freezing temperature upon gradually cooling the liquid.

This brief discussion demonstrates that it is entirely meaningless to correlate spectral positions with bond distances using a database composed of different chemical compounds and to compare the strength of hydrogen bonds of systems while disregarding their exact thermodynamic state. We will address the issue of defining a proper $\tilde{\nu}(\langle r\rangle)$ correlation from temperature- and density-dependent linear IR absorption spectra in a future publication. Suffice it to mention at this stage that the above features may indeed characterize ammonia as a fluid of weakly interacting particles rather than a hydrogen-bonded fluid. However, nonlinear spectroscopy (e.g., femtosecond midinfrared pump-probe or ultrafast multidimensional IR spectroscopy) as a function of temperature and density[28,29] is required to further substantiate such a premature interpretation.

Vibrational structure of the solute

The monodeuteration lifts the twofold degeneracy of the antisymmetric stretching and deformation modes of NH_3 and results in pairs of stretching or deformation fundamentals whose components have either a_1 or b_2 vibrational symmetry; i.e., they are either symmetric or antisymmetric with respect to the C_s plane of symmetry of the monodeuterated ammonia. In the gas phase,[32,33] the NH-stretching frequencies of our solute are $\nu_{3a} = 3366$ cm^{-1} and $\nu_{3b} = 3439$ cm^{-1}. Because of their high frequencies, these vibrations play the role of spectator modes only since the solute is initially excited to the lower-lying first excited state of the ND-stretching mode. Their pure vibrational manifolds are, therefore, irrelevant for the studies reported here.

Of more importance may be the lower-lying bending fundamentals,[32,33] which are found in the gas phase at $\nu_{4a} = 1598$ cm^{-1} and $\nu_{4b} = 1390$ cm^{-1}. Together with the "um-

brella" fundamental,[32,33] ν_2, whose gas-phase resonance is located at 886 cm^{-1}, these vibrational states may potentially serve as intermediates and can be transiently populated following an initial ND-stretching excitation.

Referring to Fig. 1, the experimental mid-IR absorption spectra display a pronounced asymmetry with a long tail toward the lower frequencies. This feature is likely due to residual absorptions from the deuterium-richer isotopomer, NHD_2, which is also present in the fluid mixture to very low concentrations because of the rapid isotope exchange. Indeed, in the highly diluted gas phase, the symmetric component of the ND-stretching mode, ν_{3a}, of the bideuterated isotopomer[32,33] is redshifted by only 73 cm^{-1} as compared to the ND-stretching fundamental, ν_1, of our solute of interest. This frequency difference drops to 50–60 cm^{-1} in going from the gas phase into a cryogenic inert gas matrix.[34] The antisymmetric component, ν_{3b}, of NHD_2, on the other hand, is blueshifted in the gas phase[32,33] by just 54 cm^{-1} relative to ν_1 of the solute. This value remains almost unchanged when the solute is embedded in a cryogenic matrix.[34]

An analysis of the experimental spectra in terms of a superposition of various conventional line shapes such as Gaussian, Lorentzian, and/or Voigt profiles yields unsatisfactory fitting results. This might be interpreted by contributions from line broadening mechanisms for the fluid system, which are considerably more complex as compared to those typical for the gas phase or low-temperature noble gas matrices. At any rate, using statistical arguments, the molar ratio NHD_2/NH_2D can be estimated to be well below 5% for the samples prepared for this study. Hence, the influence of the doubly deuterated isotopomer on the mid-IR pump-probe spectroscopy discussed below is insignificant.

The fundamental frequencies of the solvent species NH_3 occupy entirely different spectral regions:[32,33] the famous umbrella mode, ν_2, is located at 933 cm^{-1}, the doubly degenerate antisymmetric bending, ν_4, has its resonance at 1626 cm^{-1}, and the symmetric and (doubly degenerate) antisymmetric stretches are found at $\nu_1=3336$ cm^{-1} and at $\nu_3=3443$ cm^{-1}, respectively. Nevertheless, there is significant IR activity of NH_3 in the ND-stretching region. In a cryogenic Ne matrix,[34] a transition was found at 2465 cm^{-1}, which was assigned to a combination band involving the umbrella mode and the antisymmetric bending vibration of the molecule, i.e., $(\nu_2+\nu_4)$. If this assignment is correct, the off-diagonal anharmonicity between these two intramolecular solvent modes is surprisingly large, i.e., −94 cm^{-1}.

All these spectroscopic data are summarized in the energy level scheme depicted in Fig. 2 and hint at possible relaxation pathways (wavy arrows) for intermolecular energy transfer between the NH_2D solute and the NH_3 solvent following an initial excitation of the solute's ND-stretching vibration. One possible scenario involves the direct transfer of vibrational energy from the initially prepared symmetric stretch ν_1 of the solute onto the $(\nu_2+\nu_4)$ combination of a neighboring NH_3 solvent particle. Provided the gas-phase energetics also hold for the denser fluid, this transfer appears to be fully resonant because the energy mismatch between the two vibrational excitations is only 41 cm^{-1}, i.e., well within a thermal excitation. Once the energy is deposited into

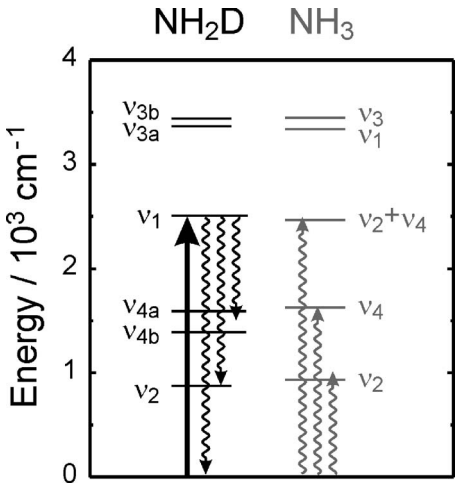

FIG. 2. Energy level diagram for the vibrational manifolds of NH_2D (left) and of NH_3 (right, in gray). The vertical arrow indicates the pump transition on the ND-stretching mode of the solute. The wavy arrows indicate possible intramolecular energy transfer pathways that are resonant with excitations of the solvent.

an intramolecular mode of a nearby solvent molecule, it will rapidly make its way into the bulk by delocalization among other NH_3 molecules where it will eventually fully thermalize.

Alternatively, from the gas-phase data, the energy gap between ν_1 and ν_{4a} (ν_{4b}) of the solute can be calculated to be 915 (1116) cm^{-1}. These values nearly coincide with the umbrella fundamental of the solvent molecules, suggesting that the pathway ν_1 (solute) $\rightarrow \nu_4$ (solute) $+\nu_2$ (solvent) for direct vibrational energy transfer is also fully resonant within the thermal excitations, provided the gas-phase and fluid-phase energetics are similar.

Finally, an intramolecular transition of the solute from its initially populated ν_1 state to the first excited state of its own umbrella mode requires the uptake of 1630 cm^{-1} of energy by a solvent molecule. As can be seen in Fig. 2, such a process is also easily facilitated by the transfer of excitation to the antisymmetric fundamental of a neighboring NH_3. Hence, a pathway ν_1 (solute) $\rightarrow \nu_2$ (solute) $+\nu_4$ (solvent) is also fully resonant even in the gas phase.

So far, we have only discussed transitions between vibrational fundamentals. However, we can already anticipate that the first overtone of umbrella mode of the solute will be located near its two NH deformation fundamentals assuming ordinary diagonal anharmonicities. Therefore, a transfer path according to ν_1 (solute) $\rightarrow 2\nu_2$ (solute) $+\nu_2$ (solvent) can also be easily envisioned. It may even be of higher impact as compared to ν_1 (solute) $\rightarrow \nu_4$ (solute) $+\nu_2$ (solvent) for symmetry reasons.

The initially excited ND-stretching mode involves motion primarily within the C_s symmetry plane. In contrast to the umbrella mode, which includes in-plane motion of the deuteron with respect to C_s of the solute, the pairs of NH-stretching and NH-deformation modes involve predominantly out-of-plane motions of the hydrogens. As a consequence, the transition matrix elements for vibrational relaxation through the umbrella manifold of the solute may be much larger as compared to those for other relaxation pathways.

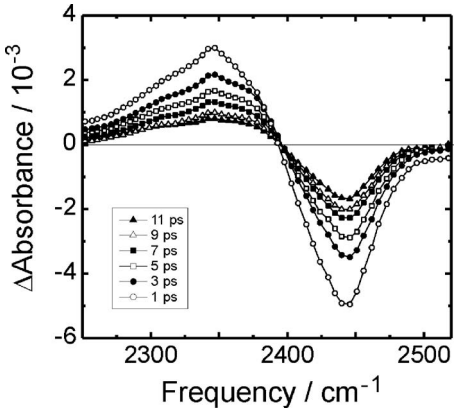

FIG. 3. Transient differential absorbance spectra of NH_2D dissolved in NH_3 for various pump-probe time delays following an initial ND-stretching excitation with femtosecond pulses centered at 2450 cm^{-1}. The solute concentration was 6 mol % and the sample was kept at 233 K and 1050 bar, corresponding to a solvent density of 43 mol/l.

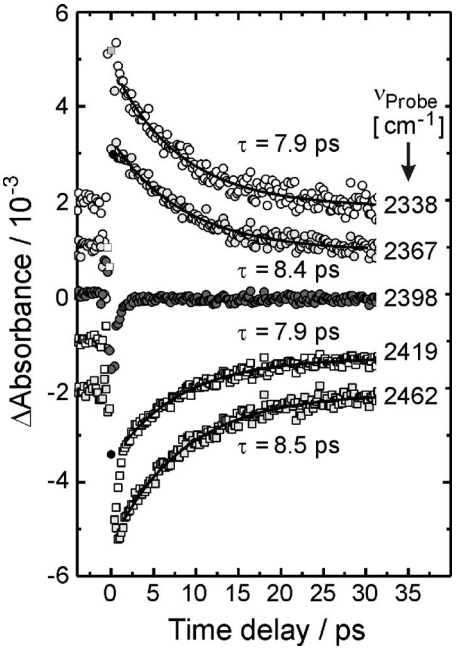

FIG. 4. Time-resolved pump-induced absorbance traces of NH_2D dissolved in NH_3 for various probe wavelengths following an initial ND-stretching excitation with femtosecond pulses centered at 2450 cm^{-1}. The solute concentration was 6 mol % and the sample was kept at 233 K and 1050 bar, corresponding to a solvent density of 43 mol/l. For clarity, the traces were successively shifted by an increment of 10^{-3} differential absorbance unit. The solid curves represent fits of the data to a single-exponential decay.

Femtosecond pump-probe spectroscopy

Figure 3 displays transient differential (i.e., pump-induced) absorbance spectra of a 6 mol % solution of NH_2D in NH_3 at a temperature of 233 K and a pressure of 1050 bar corresponding to a mass density of 0.73 g/cm^3 or equivalently, 43 mol/l. The data were obtained with pump pulses centered at 2450 cm^{-1}. A ground-state bleach corresponds to negative differential absorbances, while a transient absorption gives rise to positive signals. Weak spectral modulations around a probe frequency of 2350 cm^{-1} are caused by atmospheric absorptions of our laser pulses by residual CO_2 and are, therefore, artificial.

Because the spectral bandwidth of our excitation pulses covers the entire ND-stretching resonance, the ground-state bleach peaks exactly at the frequency of maximal absorbance in the linear mid-IR spectrum recorded under identical thermodynamic conditions, i.e., at 2445 cm^{-1}. The maximum of the transient absorption due to the excited ND-stretching state occurs at a probe frequency of 2348 cm^{-1}. Thus, the apparent redshift of the transient absorption relative to the ground-state bleach is roughly twice as large as the bandwidth of the linear ground-state absorption, which allows us to estimate the diagonal anharmonicity, $\Delta(\nu_1)$, for the ND-stretching vibration of the solute directly from the frequency offset between these two components to the pump-induced spectrum. Inspection of the spectrum in Fig. 3 leads to a value for $\Delta(\nu_1)$ of roughly -97 cm^{-1}, which compares rather well with an anharmonicity of -77 cm^{-1} as predicted for NH_2D from an early *ab initio* quartic force field by Martin *et al.* using coupled cluster theory.[42]

From Fig. 3, it can further be seen that the excited-state absorption decays on a time scale of 10 ps under the given thermodynamic conditions. Likewise, the ground-state bleach recovers on an identical time scale, thereby giving rise to a pronounced isosbestic point at a probe frequency of 2398 cm^{-1}. From this observation, we can immediately conclude that the depopulation of the ND-stretching excited state is the rate-determining step for vibrational energy transfer back to the ground state. Any intermediate state through which the energy may transiently flow is likely to live much shorter than the initially excited ND-stretching state and can, therefore, never be significantly populated during relaxation.

Furthermore, it can be concluded that under the given thermodynamic conditions, vibrational spectral diffusion within the ND-stretching resonance of NH_2D in NH_3 is much faster than vibrational energy relaxation. If these two distinct dynamical processes occur on similar time scales, the spectral shape of the pump-induced absorbance should vary with the pump-probe time delay.[43] This is clearly not observed in our data.

To elucidate in more detail the intermediate states through which the energy flows and to map out the various couplings between the various modes involved in vibrational relaxation, two-color experiments similar to those previously performed by us[36,44] and others[45,46] on liquid water are highly desirable. Unfortunately, the limited transparency range of the sapphire windows of our high-pressure sample cell precludes measurements which pump and/or probe the bending degrees of freedom of our solute because these modes absorb well below 1600 cm^{-1}. In light of this technical limitation, one can only refer to Fig. 2 at this stage, which renders mechanisms involving ν_2 and ν_4 states of the solutes as the most intuitive resonant energy transfer pathways.

To quantify the dynamics of vibrational relaxation more accurately, the pump-induced differential absorbance is plotted in Fig. 4 as a function of pump-probe time delay for various probe frequencies. Consistent with an isosbestic point, no temporal evolution can be recorded at 2398 cm^{-1} except for a coherent artifact from the cell windows around a pump-probe time delay of zero. Both the ground-state bleach and the anharmonically shifted absorption decay are in con-

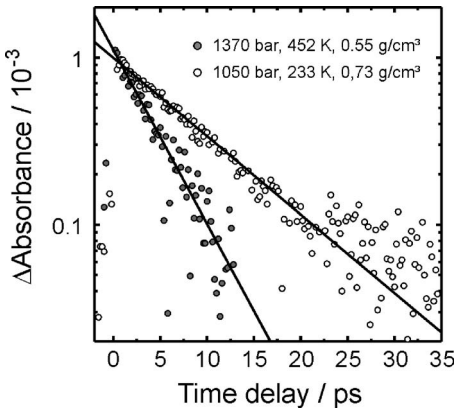

FIG. 5. Semi-logarithmic plot of the pump-induced excited-state absorption of NH_2D in NH_3 following an initial ND-stretching excitation with femtosecond pulses centered at 2450 cm^{-1}. The data were recorded for two different thermodynamic conditions. The solid lines represent fits of the data to a single-exponential decay with time constants of 8.5 and 4.5 ps, respectively.

cert in a single exponential fashion. Monoexponential fits (solid curves in Fig. 4) clearly reveal identical time constants of around 8 ps for both signal components as expected if the excited-state decay is rate limiting.

The monoexponential behavior of the excited-state decay is emphasized once again in Fig. 5 by a semilogarithmic plot of the pump-induced absorbance versus the time delay. The same figure also highlights the dependence of the relaxation kinetics and the lifetime of the ND-stretching excited state on the temperature. The two transients were recorded roughly at similar densities. Obviously, with increasing temperature, vibrational energy transfer accelerates. This temperature dependence is in stark contrast to the isobaric and isochoric temperature dependences we recently reported for the vibrational energy relaxation dynamics of HOD in liquid-to-supercritical D_2O.[28,29] In the case of water, vibrational relaxation becomes faster upon cooling. This is because with decreasing temperature, the average number of hydrogen bonds per water molecule increases for a given bulk density. The temperature dependence of the energy transfer kinetics observed in Fig. 5 for NH_2D in ammonia is much more reminiscent of a solute vibrationally relaxing in a nonassociating fluid.

Numerical simulations

To test this interpretation, we analyzed the density and temperature dependence of the ND-stretching relaxation rate of NH_2D in NH_3 in terms of a simple "breathing sphere" model consisting of a spherically symmetric oscillator (solute) embedded in a Lennard-Jones bath (solvent). Such a model has been used previously in numerous studies to predict the density dependence of vibrational energy relaxation rates of diatomic[47] and polyatomic molecules.[48] According to Landau-Teller theory,[49–52] the classical relaxation rate coefficient is given by

$$k = \frac{1}{2\mu k_B T} S_F(\omega_0), \tag{1}$$

where μ is the reduced mass of the oscillator and ω_0 is its vibrational frequency. The Boltzmann constant is denoted as k_B and T is the temperature. In Eq. (1), $S_F(\omega_0)$ represents the power spectrum of the fluctuating forces $F(t)$ exerted by the solvent onto the excited vibration of the solute. The latter, in turn, is held rigid at its equilibrium displacement, σ_0. The spectral density can be calculated from the cosine transform of the force-force time-correlation function according to

$$S_F(\omega) = \int_{-\infty}^{+\infty} dt \cos(\omega t) \langle F(0)F(t) \rangle. \tag{2}$$

In practice, $F(t)$ is computed from a classical molecular dynamics (MD) simulation.

The vibrational coordinate of the breathing sphere is its diameter $\sigma_{BS}=\sigma_0+q$, where q describes the displacement from the equilibrium value. When the breathing sphere collides with a bath particle of diameter σ_s, the interaction is determined by the effective diameter $(\sigma_s+\sigma_0+q)/2$. Then, the perturbing force acting on the vibrational coordinate is given by

$$F = \sum_i f(r_i) = -\sum_i \left. \frac{\partial V(r_i,q)}{\partial q} \right|_{q=0}, \tag{3}$$

where $V(r,q)$ is the interaction potential, $f(r)$ denotes the binary force, and the summation is performed over all the bath particles. Considering only Lennard-Jones interactions between the breathing sphere and its bath, the binary force on the vibrational coordinate can be written as[47]

$$f(r) = -12\frac{\varepsilon}{\sigma}\left[2\left(\frac{\sigma}{r}\right)^{12} - \left(\frac{\sigma}{r}\right)^{6}\right]. \tag{4}$$

The effective interaction parameters are given by $\sigma=(\sigma_s+\sigma_0)/2$ and $\varepsilon=(\varepsilon_s\varepsilon_0)^{1/2}$, where ε_s and ε_0 are the solvent-solvent and solute-solute well depths. For our simulations, we simplify the model by considering the special case of a neat liquid, i.e., the small mass difference between NH_3 and NH_2D is neglected. Furthermore, the Lennard-Jones parameters obey the equalities $\varepsilon_s=\varepsilon_0=\varepsilon$ and $\sigma_s=\sigma_0=\sigma$. This procedure improves the statistics of the molecular dynamics simulations considerably because each solvent particle can now be treated as a solute also. The interaction parameters $\sigma=0.3346$ nm and $\varepsilon/k_B=309.5$ K are chosen such that the critical data of the Lennard-Jones fluid ($T_c^*=k_BT_c/\varepsilon=1.31$ and $\rho_c^*=\rho_c\sigma^3=0.31$)[53] match those of NH_3 ($T_c=405.5$ K and $\rho_c=0.234$ g/cm^3).[37]

The MD simulations were performed in a cubic simulation box with periodic boundary conditions containing 500 particles as described previously.[54,55] Using the leapfrog algorithm, the equations of motions were integrated with a time step of $\Delta t=4$ fs. After equilibration, the breathing sphere force $F_i(t)$ acting on each particle i was recorded for 2^{19} time steps. The power spectrum was calculated as follows. First, the entire time series was divided into overlapping segments, each of which had a length of 2^{14} time steps and neighboring segments overlapped for 75% of their tem-

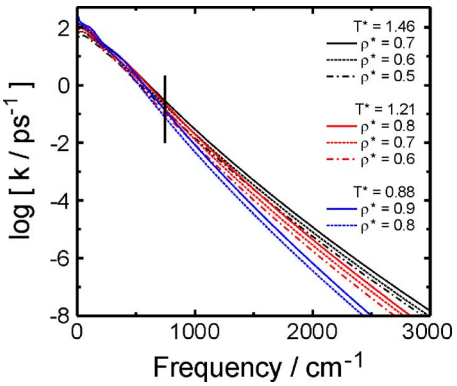

FIG. 6. (Color online) Frequency-dependent Landau-Teller rate coefficients for vibrational energy transfer of NH_2D in NH_3 for various reduced densities, $\rho^* = \rho\sigma^3$, and reduced temperatures, $T^* = k_B T/\varepsilon$. The actual temperatures are 452 K (black), 373 K (red), and 273 K (blue). The vertical bar indicates the breathing sphere frequency that results in the best agreement between simulation and experiment.

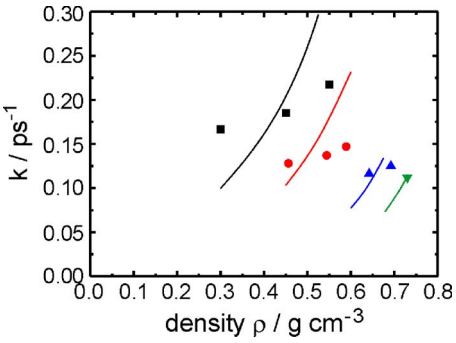

FIG. 7. (Color online) Comparison of the density- and temperature-dependent experimental rate coefficients for vibrational energy relaxation of NH_2D in NH_3 (symbols) with the Landau-Teller rate constants obtained at a breathing sphere frequency of 745 cm^{-1} (solid curves). The temperatures are 452 K (black), 373 K (red), 273 K (blue), and 233 K (green) in both the simulation and the experiments.

poral length. Then, each segment was multiplied with a Hanning window function and the above power spectrum was computed from the segment's force-force correlation function [Eq. (1)] using the Wiener-Khintchine theorem. Finally, an averaging of the spectral density was carried out over all segments and all particles.

Figure 6 shows frequency dependent relaxation rates obtained from such MD simulations together with Eq. (1). The individual spectra are characterized by a stretched exponential shape.[54,55] For a given temperature, the relaxation rate grows with increasing density regardless of the oscillator frequency. This increase is essentially caused by the density dependence of the collision frequency. At constant density, an increasing temperature leads to a faster relaxation because the collisions become harder as the underlying fluctuating forces progressively acquire higher frequency components. This temperature effect becomes more pronounced with increasing frequency of the relaxing oscillator.

So far, the frequency, ν_0, of the breathing sphere oscillator has not yet been specified explicitly. Note that this frequency corresponds to the quantum mechanical energy gap between the initial and the final vibrational states of the relaxing solute. Here, we empirically determined ν_0 by comparing the calculated relaxation rates with those obtained experimentally. A value of 745 cm^{-1} (see the vertical bar in Fig. 1) results in a reasonable agreement between the simulation and the pump-probe data described above. The corresponding density- and temperature-dependent rate constants are shown in Fig. 7 together with the rate coefficients obtained from the decay of the anharmonically shifted transient absorption of the ND-stretching excited state of NH_2D in NH_3.

It is tempting to interpret the breathing sphere frequency with a particular resonant energy transfer pathway such as those sketched in Fig. 2. A value for ν_0 of 745 cm^{-1} comes indeed rather close to the energy gap of 915 cm^{-1} between ν_1 and ν_{4a} (ν_{4b}) of the solute. However, it is important to emphasize that our simulations were carried out on a fluid consisting of structureless and rigid Lennard-Jones particles. Hence, the breathing sphere frequency becomes entirely meaningless. Only if a flexible model for NH_3 is used that takes into account realistic vibrational degrees of freedom of the solute and the solvent can the spectral density exhibit pronounced resonance peaks that result from solute energy gaps quantitatively matching those of the solvent. Such calculations are indeed highly valuable in unraveling the detailed energy transfer mechanism and are currently being performed on fluid ammonia in our laboratories.

Inspection of Fig. 7 reveals that our simple breathing sphere model is able to reproduce the temperature dependence of the rate constant quite nicely. This confirms that the influence of hydrogen bonding on the dynamics of vibrational energy relaxation in fluid ammonia is indeed minor.

However, the simulations are not able to reproduce the density dependence for a given temperature in a satisfactory manner. Although the model simulations yield a positive curvature of $k(\rho)$ in agreement with the experimental data, they result in a much steeper overall density dependence. Moreover, the density dependence of the experimental rate constant must be significantly more complex than it might appear at a first glance. This is because k must be equal to zero for vanishing solvent density; however, the data seem to extrapolate to a nonphysical finite intercept for all temperatures.

Therefore, the function $k(\rho)$ that describes the density dependence of the ND-stretching relaxation of NH_2D in NH_3 correctly must have an inflection point at sufficiently low densities (e.g., $\rho \leqslant 0.3$ for 453 K). Such an S-shaped behavior was indeed found for the vibrational relaxation of polyatomic molecules dissolved in supercritical nonpolar fluids.[46] This peculiar feature was traced back to the evolution of the local solvent density obtained from the first maximum of the solute-solvent radial distribution function with increasing bulk density and can only show up for unlike solute-solvent combinations with attractive solutes. Therefore, local density effects cannot be held responsible for the deviations seen in Fig. 7 because the system under investigation here is essentially a neat liquid.

We believe that the rather weak density dependence compared to the simulations is brought about by detuning effects or, equivalently, energetic shifting of vibrational states of the solvent. By increasing the density, the acceptor

energy gap on the solvent particles is shifted out of resonance with increasing density, thereby effectively decelerating the apparent rate for energy transfer. We will further pursue this explanation in future molecular dynamics simulations that are based on more realistic and flexible model potentials for fluid ammonia.

In summary, we have presented the first femtosecond mid-IR study aimed at elucidating the dynamics of vibrational energy relaxation in liquid-to-supercritical ammonia. The density and temperature dependence of the energy transfer rates suggests that contrary to water, hydrogen bonding does not significantly affect the relaxation dynamics in NH_3. Rather, a comparison with classical Landau-Teller rate constants obtained from molecular dynamics simulations suggests that the energy transfer is dominated by weak Lennard-Jones-type solute solvent interactions.

ACKNOWLEDGMENTS

We gratefully acknowledge financial support by the Deutsche Forschungsgemeinschaft, Grant No. VO-593/5-1, and the Fonds der Chemischen Industrie (T.S.).

[1] P. Schuster, G. Zundel, and C. Sandorfy, *The Hydrogen Bond: Recent Developments* (North Holland, Amsterdam, 1976).
[2] *The Physics and Physical Chemistry of Water*, edited by F. Franks (Plenum, New York, 1972), Vol. 1.
[3] I. Olovsson and D. H. Templeton, Acta Crystallogr. **12**, 832 (1959).
[4] R. Boese, N. Niederprum, D. Blaser, A. Maulitz, M. Y. Antipin, and P. R. Mallinson, J. Phys. Chem. B **101**, 5794 (1997).
[5] D. D. Nelson, Jr., G. T. Fraser, and W. Klemperer, J. Chem. Phys. **83**, 6201 (1985).
[6] E. H. T. Olthof, A. van der Avoird, P. E. S. Wormer, J. G. Loeser, and R. J. Saykally, J. Chem. Phys. **101**, 8443 (1994).
[7] W. Klopper, Mol. Phys. **96**, 559 (1999).
[8] J. J. Novoa and C. Sosa, J. Phys. Chem. **99**, 15837 (1995).
[9] C. J. Wormald and B. Wurzberger, J. Chem. Thermodyn. **33**, 1193 (2001).
[10] A. H. Narten, J. Chem. Phys. **66**, 3117 (1977).
[11] F. Sette, G. Ruocco, A. Cunsolo, C. Masciovecchio, G. Monaco, and R. Verbeni, Phys. Rev. Lett. **84**, 4136 (2000).
[12] P. Giura, R. Angelini, F. Datchi, G. Ruocco, and F. Sette, J. Chem. Phys. **127**, 084508 (2007).
[13] P. Chieux and H. Bertagnolli, J. Phys. Chem. **88**, 3726 (1984).
[14] T. Bausenwein, H. Bertagnolli, A. David, K. Goller, H. Zweier, K. Todheide, and P. Chieux, J. Chem. Phys. **101**, 672 (1994).
[15] H. Thompson, J. C. Wasse, N. T. Skipper, S. Hayama, D. T. Bowron, and A. K. Soper, J. Am. Chem. Soc. **125**, 2572 (2003).
[16] M. Buback, Ber. Bunsenges. Phys. Chem. **78**, 1230 (1974).
[17] M. Schwartz and C. H. Wang, J. Chem. Phys. **59**, 5258 (1973).
[18] M. Bradley, T. W. Zerda, and J. Jonas, J. Chem. Phys. **82**, 4007 (1985).
[19] M. A. Ricci, M. Nardone, F. P. Ricci, C. Andreani, and A. K. Soper, J. Chem. Phys. **102**, 7650 (1995).
[20] A. D. Boese, A. Chandra, J. M. L. Martin, and D. Marx, J. Chem. Phys. **119**, 5965 (2003).
[21] A. Tongraar, T. Kerdcharoen, and S. Hannongbua, J. Phys. Chem. A **110**, 4924 (2006).
[22] E. T. J. Nibbering and T. Elsaesser, Chem. Rev. (Washington, D.C.) **104**, 1887 (2004).
[23] C. J. Fecko, J. D. Eaves, J. J. Loparo, A. Tokmakoff, and P. L. Geissler, Science **301**, 1698 (2003).
[24] K. Winkler, J. Lindner, H. Bürsing, and P. Vöhringer, J. Chem. Phys. **113**, 4674 (2000).
[25] K. Winkler, J. Lindner, and P. Vöhringer, Phys. Chem. Chem. Phys. **4**, 2144 (2002).
[26] S. Woutersen, U. Emmerich, and H. J. Bakker, Science **278**, 658 (1997).
[27] M. L. Cowan, B. D. Bruner, N. Huse, J. R. Dwyer, B. Chugh, E. T. J. Nibbering, T. Elsaesser, and R. J. D. Miller, Nature (London) **434**, 199 (2005).
[28] D. Schwarzer, J. Lindner, and P. Vöhringer, J. Chem. Phys. **123**, 16105 (2005).
[29] D. Schwarzer, J. Lindner, and P. Vöhringer, J. Phys. Chem. A **110**, 2858 (2006).
[30] K. K. Lehmann and S. L. Coy, J. Chem. Soc., Faraday Trans. 2 **84**, 1389 (1988).
[31] E. Kauppi and L. Halonen, J. Chem. Phys. **103**, 6861 (1995).
[32] M. Snels, H. Hollenstein, and M. Quack, J. Chem. Phys. **119**, 7893 (2003).
[33] M. Snels, H. Hollenstein, and M. Quack, J. Chem. Phys. **125**, 194319 (2006).
[34] M. E. Jacox and W. E. Thompson, J. Mol. Spectrosc. **228**, 414 (2004).
[35] A. J. Lock and H. J. Bakker, J. Chem. Phys. **117**, 1708 (2002).
[36] J. Lindner, P. Vöhringer, M. S. Pshenichnikov, D. Cringus, D. A. Wiersma, and M. Mostovoy, Chem. Phys. Lett. **421**, 329 (2006).
[37] W. S. Groenier and G. Thodos, J. Chem. Eng. Data **5**, 285 (1960).
[38] L. Abouaf-Marguin, M. E. Jacox, and D. E. Milligan, J. Mol. Spectrosc. **67**, 34 (1977).
[39] A. Loutellier and J. P. Perchard, J. Mol. Struct. **198**, 51 (1989).
[40] B. Nelander, Chem. Phys. **87**, 283 (1984).
[41] A. Novak, Struct. Bonding (Berlin) **18**, 177 (1974).
[42] J. M. L. Martin, T. J. Lee, and P. R. Taylor, J. Chem. Phys. **97**, 8361 (1992).
[43] H. J. Bakker, H. K. Nienhuys, G. Gallot, N. Lascoux, G. M. Gale, J. C. Leicknam, and S. Bratos, J. Chem. Phys. **116**, 2592 (2002).
[44] J. Lindner, D. Cringus, M. S. Pshenichnikov, and P. Vöhringer, Chem. Phys. **341**, 326 (2007).
[45] S. Ashihara, N. Huse, A. Espagne, E. T. J. Nibbering, and T. Elsaesser, J. Phys. Chem. A **111**, 743 (2007).
[46] L. Chieffo, J. Shattuck, J. J. Amsden, S. Erramilli, and L. D. Ziegler, Chem. Phys. **341**, 71 (2007).
[47] S. A. Egorov and J. L. Skinner, J. Chem. Phys. **105**, 7047 (1996).
[48] V. S. Vikhrenko, D. Schwarzer, and J. Schroeder, Phys. Chem. Chem. Phys. **3**, 1000 (2001).
[49] R. Zwanzig, J. Chem. Phys. **34**, 1931 (1961).
[50] R. M. Whitnell, K. R. Wilson, and J. T. Hynes, J. Phys. Chem. **94**, 8625 (1990).
[51] S. A. Adelman, R. Muralidhar, and R. H. Stote, J. Chem. Phys. **95**, 2738 (1991).
[52] M. Tuckerman and B. J. Berne, J. Chem. Phys. **98**, 7301 (1993).
[53] J. J. Potoff and A. Z. Panagiotopoulos, J. Chem. Phys. **109**, 10914 (1998).
[54] D. Schwarzer and M. Teubner, J. Chem. Phys. **116**, 5680 (2002).
[55] M. Teubner and D. Schwarzer, J. Chem. Phys. **119**, 2171 (2003).